Far East Journal of Applied Mathematics

http://www.pphmj.com
http://dx.doi.org/10.17654/AM096060307
Volume 96, Number 6, 2017, Pages 307-321 **ISSN: 0972-0960**

EFFECTS OF THERMAL RADIATION ON PERISTALTIC TRANSPORT OF A COUPLE STRESS FLUID IN TAPERED ASYMMETRIC CHANNEL

S. Sheeba Juliet[1], M. Vidhya[2], E. P. Siva[3] and A. Govindarajan[3]

[1]Department of Mathematics
C. S. I. Ewart Women's Christian College
Sathyabama University
Melrosapuram 603 204, India

[2]Department of Mathematics
Sathyabama University
Sholinganallur 600 119, India

[3]Department of Mathematics
SRM University
Kattankulathur 603 203
Tamil Nadu, India

Abstract

This paper describes the effect of the thermal radiation on peristaltic transportation of a couple stress fluid in an asymmetric channel in the

Received: October 5, 2016; Accepted: May 6, 2017
2010 Mathematics Subject Classification: 74F10, 74F05, 80A20.
Keywords and phrases: peristalsis, couple stress, thermal radiation, tapered asymmetric channel.

presence of external magnetic field. The governing equations are reduced by using very low Reynolds number and long-wavelength rough calculations. Closed-form analytical expressions for axial velocity and temperature distribution have been obtained. Graphs are presented and analyzed for various parameters involved in the problem.

Introduction

The peristaltic flow has been a focus of scientific study during the past few decades but in recent years it has established much attention due to its wide applications in manufacturing engineering and physiology. Few applications of the peristaltic mechanism include the urine transport from a kidney to the bladder and the transport of the spermatozoa in the cervical canal, the chime movement in the large intestine. Numerous theoretical and experimental studies have been conducted to understand the peristaltic action after the first study of Latham [1]. The pre-results of the testing were in good agreement with the theoretical results of Shapiro et al. [2]. Then, Burns and Parkes [3] have studied the peristaltic motion of a viscous fluid through the channel. Detailed discussions of the peristaltic flow under various assumptions have been presented in the studies [4-7] (several references therein).

The progress in the theory of peristaltic transport with heat transfer was given in [8-12]. The examination of heat transfer is of huge value in dilution method in examining blood flow and biological tissues, etc. The effect of mass and heat transfer on the MHD peristaltic transport of viscous fluid has been examined in the studies [13, 14]. Eldabe et al. [15] have employed the convective boundary conditions with mass and heat transfer on peristaltic transport. Mass and heat transfer effects on magnetohydrodynamics peristaltic flow through a porous medium with asymmetric flexible walls were discussed by Srinivas and Kothandapani [16].

Couple stress fluid is useful in learning some physical problems for the reason that it acquires the mechanism to depict rheological fluids such as oil containing a small quantity of high polymer chemical addition, liquid crystals etc. Stokes [17] formulated to predict microstructural characteristics (particle size) of physiological suspensions with good precision. Mekheimer [18] studied the problem in the peristalsis of a couple stress fluid in an asymmetric channel. The MHD peristaltic transport of a couple stress fluid in an asymmetric channel was observed by Nadeem and Akram [19] and Mekheimer [20].

It is noted that the intra uterine fluid flow in a sagittal uterus cross-section releases a channel enclosed by two parallel walls having different amplitudes and phase difference. Several authors have discussed the intra uterine transport [21-25].

The peristaltic flow of a coupled stress fluid through a porous asymmetric channel is considered. The flow equations are reduced under large wavelength and less Reynolds number. The closed-forms of temperature and velocity distribution are obtained. The effects of various parameters on fluid flow are discussed through graphs.

Mathematical Formulation

The flexible tapered asymmetric channel filled with porous medium is considered. The channel walls are given by

$$H_2(X, t') = d + m'X + b_2 \sin\frac{2\pi}{\lambda}(X - ct'), \tag{1}$$

$$H_1(X, t') = -d - m'X - b_1 \sin\left[\frac{2\pi}{\lambda}(X - ct') + \varphi\right], \tag{2}$$

where b_1 and b_2 are the amplitudes of walls, d is the semi-average width of the channel, λ is the wavelength, $m'(m' << 1)$ is the parameter of non-uniform. b_1, b_2, d and φ satisfy the following condition:

$$b_1^2 + b_2^2 + 2b_1b_2 \cos(\varphi) \leq (2d)^2, \tag{3}$$

where T_0 - temperature of the lower wall and the temperature at the upper wall is T_1. The governing equations of continuity and momentum are given as follows:

$$\frac{\partial U}{\partial X} + \frac{\partial V}{\partial Y} = 0, \tag{4}$$

$$\rho\left[\frac{\partial U}{\partial t'} + U\frac{\partial U}{\partial X} + V\frac{\partial U}{\partial Y}\right] = -\frac{\partial P}{\partial X} + \mu\nabla^2 U - \eta\nabla^4 U, \tag{5}$$

$$\rho\left[\frac{\partial V}{\partial t'} + U\frac{\partial V}{\partial X} + V\frac{\partial V}{\partial Y}\right] = -\frac{\partial P}{\partial Y} + \mu\nabla^2 V - \eta\nabla^4 V, \tag{6}$$

$$\rho C_p\left[\frac{\partial T}{\partial t'} + U\frac{\partial T}{\partial x} + V\frac{\partial T}{\partial Y}\right] = \kappa\left[\frac{\partial^2 T}{\partial X^2} + \frac{\partial^2 T}{\partial Y^2}\right]$$
$$+ \mu\left\{2\left[\left(\frac{\partial U}{\partial X}\right)^2 + \left(\frac{\partial V}{\partial Y}\right)^2\right] + \left(\frac{\partial U}{\partial Y} + \frac{\partial V}{\partial X}\right)^2\right\} - \frac{\partial q_r}{\partial Y}, \tag{7}$$

where U and V are the velocities in X and Y directions, t' is the time, μ is the viscosity, ρ is the fluid density, C_p is the specific heat, P is the pressure, T is the temperature, η is the constant associated with couple stress, κ is the thermal conductivity and q_r is the radiative heat flux.

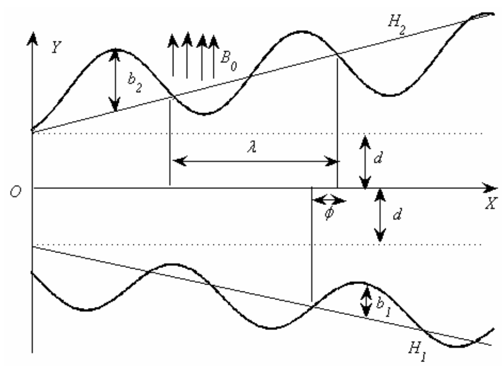

Figure 1. Tapered flexible walls diagram.

By using Rosseland approximation for radiation, the radiative heat flux q_r is given by

$$q_r = -\frac{16\sigma^* T_0^3}{3k^*} \cdot \frac{\partial T}{\partial Y}, \tag{8}$$

where σ^* and k^* are the Stefan-Boltzmann constant and mean absorption coefficient, respectively, and

$$\nabla^2 = \frac{\partial^2}{\partial X^2} + \frac{\partial^2}{\partial Y^2} = 0, \quad \nabla^4 = \nabla^2 \nabla^2. \tag{9}$$

Below are some non-dimensional variables:

$$x = \frac{X}{\lambda},\ y = \frac{Y}{\lambda},\ t = \frac{ct'}{\lambda},\ u = \frac{U}{c},\ v = \frac{V}{c},\ \delta = \frac{d}{\lambda},\ h_1 = \frac{H_1}{d},$$

$$h_2 = \frac{H_2}{d},\ p = \frac{d^2 P}{c\lambda\mu},\ \theta = \frac{T - T_0}{T_1 - T_0},\ a = \frac{b_1}{d},\ b = \frac{b_2}{d},\ S^2 = \frac{d^2\mu}{\eta},$$

$$R_n = \frac{16\sigma^* T_0^3}{3k^* \mu C_p}.$$

The problem statement in the dimensionless form is given by

$$R\delta\left[\frac{\partial u}{\partial t} + u\frac{\partial u}{\partial x} + v\frac{\partial u}{\partial y}\right] = -\frac{\partial p}{\partial x} + \left(\delta^2 \frac{\partial^2 u}{\partial x^2} + \frac{\partial^2 u}{\partial y^2}\right)$$

$$- \frac{1}{S^2}\left(\delta^2 \frac{\partial^2}{\partial x^2} + \frac{\partial^2}{\partial y^2}\right)\left(\delta^2 \frac{\partial^2 u}{\partial x^2} + \frac{\partial^2 u}{\partial y^2}\right), \tag{10}$$

$$R\delta^3\left[\frac{\partial v}{\partial t} + u\frac{\partial v}{\partial x} + v\frac{\partial v}{\partial y}\right] = \frac{\partial p}{\partial y} + \delta^2\left[\delta^2 \frac{\partial^2 v}{\partial x^2} + \frac{\partial^2 v}{\partial y^2}\right]$$

$$- \frac{1}{S^2}\left(\delta^2 \frac{\partial^2}{\partial x^2} + \frac{\partial^2}{\partial y^2}\right)\left(\delta^2 \frac{\partial^2 v}{\partial x^2} + \frac{\partial^2 v}{\partial y^2}\right), \tag{11}$$

$$R\delta\left[\frac{\partial \theta}{\partial t} + u\frac{\partial \theta}{\partial x} + v\frac{\partial \theta}{\partial y}\right] = \frac{1}{\Pr}\left[\delta^2 \frac{\partial^2 \theta}{\partial x^2} + \frac{\partial^2 \theta}{\partial y^2}\right]$$

$$+ E\left[2\left[\delta\left(\frac{\partial u}{\partial x}\right)^2 + \left(\frac{\partial v}{\partial y}\right)^2\right] + \left[\frac{\partial u}{\partial y} + \delta\frac{\partial v}{\partial x}\right]^2\right]$$

$$+ R_n \frac{\partial^2 \theta}{\partial y^2}, \tag{12}$$

where

$$\Pr = \frac{\rho\upsilon C_p}{\kappa}, \ R = \frac{\rho c d}{\mu} \ \text{and} \ E = \frac{c^2}{C_p(T_1 - T_0)}. \tag{13}$$

By assuming the long wavelength and low Reynolds number, we find from equations (10) to (13),

$$\frac{\partial p}{\partial x} + \frac{\partial^2 u}{\partial y^2} - \frac{1}{S^2}\frac{\partial^4 u}{\partial y^4} = 0, \tag{14}$$

$$\frac{\partial p}{\partial y} = 0, \tag{15}$$

$$\xi \frac{\partial^2 \theta}{\partial y^2} + E\left(\frac{\partial u}{\partial y}\right)^2 = 0, \tag{16}$$

where

$$\xi = R_n + \frac{1}{\Pr}, \tag{17}$$

where R - Reynolds number, p - dimensionless pressure, a and b - amplitudes of lower and upper walls, δ - wave number, m - non-uniform parameter, θ - dimensionless temperature, Pr - Prandtl number, R_n - radiation parameter, S - couple stress parameter and E - Eckert number.

The corresponding boundary conditions are:

$$u = 0, \ \frac{\partial^2 u}{\partial y^2} = 0, \ \theta = 1 \ \text{ at}$$

$$h_1(x, t) = -1 - mx - a\sin(2\pi(x-1) + \phi), \tag{18}$$

$$u = 0, \ \frac{\partial^2 u}{\partial y^2} = 0, \ \theta = 0 \ \text{ at}$$

$$y = h_2(x, t) = 1 + mx + b\sin 2\pi(x - t). \tag{19}$$

Analytical Solution of the Problem

The governing equations (14)-(16), subject to boundary conditions (18)-(19) are solved exactly for velocity (u) and temperature (θ).

(i) Velocity distribution

$$u = c_1 + c_2 y + c_3 \cosh Sy + c_4 \sinh Sy + \frac{\frac{\partial p}{\partial x} \cdot y}{2}, \tag{20}$$

where

$$c_1 = -\left[\frac{\partial p/\partial x . h_1^2}{2} + c_2 h_1 + c_3 \cosh Sh_1 + c_4 \sinh Sh_1\right],$$

$$c_2 = \frac{\left[\begin{array}{l}\frac{\partial p/\partial x.(h_1^2 - h_2^2)}{2} + c_3(\cosh Sh_1 - \cosh Sh_2) \\ + c_4(\sinh Sh_1 - \sinh Sh_2)\end{array}\right]}{(h_2 - h_1)},$$

$$c_3 = -\left[\frac{\partial p/\partial x + c_4 S^2 \sinh Sh_1}{S^2 \cosh Sh_1}\right],$$

$$c_4 = \frac{\partial p/\partial x(\cosh Sh_2 - \cosh Sh_1)}{S^2 \sinh S(h_2 - h_1)}.$$

(ii) Temperature distribution

$$\begin{aligned}\theta = {} & c_5 y + c_6 + A_1 y^2 + A_2 \cosh 2Sy + A_3 y^4 \\ & + A_4 \sinh 2Sy + A_5 \sinh Sy + A_6 y \cosh Sy \\ & + A_7 y^3 + A_8 \cosh Sy + A_9 y \sinh Sy,\end{aligned} \tag{21}$$

where

$$A_1 = -\frac{E}{\xi}\left[\frac{c_2^2}{2} - \frac{c_3^2 S^2}{4} + \frac{c_4^2 S^2}{4}\right], \quad A_2 = -\frac{E}{\xi}\left[\frac{c_3^2}{8} + \frac{c_4^2}{8}\right],$$

$$A_3 = -\frac{E\frac{\partial p}{\partial x}}{12\xi}, \quad A_4 = -\frac{Ec_3c_4}{4\xi}, \quad A_5 = -\frac{E}{\xi}\left[\frac{2c_2c_3}{S} - \frac{4c_4\frac{\partial p}{\partial x}}{S^2}\right],$$

$$A_6 = -\frac{2Ec_4\frac{\partial p}{\partial x}}{\xi S}, \quad A_7 = -\frac{Ec_2\frac{\partial p}{\partial x}}{3\xi S},$$

$$A_8 = -\frac{E}{\xi}\left[\frac{2c_2c_4}{S} - \frac{4c_3\frac{\partial p}{\partial x}}{S^2}\right], \quad A_9 = -\frac{2Ec_3\frac{\partial p}{\partial x}}{S\xi},$$

$$A_{10} = 1 - \begin{bmatrix} A_1h_1^2 + A_2\cosh 2Sh_1 + A_3h_1^2 + A_4\sinh 2Sh_1 \\ + A_5\sinh Sh_1 + A_6h_1\cosh Sh_1 + A_7h_1^3 \\ + A_8\cosh Sh_1 + A_9h_1\sinh Sh_1 \end{bmatrix},$$

$$A_{11} = -\begin{bmatrix} A_1h_2^2 + A_2\cosh 2Sh_2 + A_3h_2^2 + A_4\sinh 2Sh_2 \\ + A_5\sinh Sh_2 + A_6h_2\cosh Sh_2 + A_7h_2^3 \\ + A_8\cosh Sh_2 + A_9h_2\sinh Sh_2 \end{bmatrix},$$

$$c_5 = \frac{A_{10} - A_{11}}{(h_1 - h_2)}, \quad c_6 = A_{11} - c_5h_2.$$

Results and Discussion

This section details the behavior of the various parameters on axial velocity (u) and temperature distribution (θ).

Flow characteristics

Figures 2-5 show the behavior of couple stress parameter (S), a non-uniform parameter (m), phase shift (φ) and amplitude of the lower wall (a) on the axial velocity u. Figure 2 shows that an increase in S causes increase in velocity u. The amplitude of the lower wall (a) effect on u is sketched in

Figure 3. It is shown that the axial velocity increases with an increase in *a*. The effect of non-uniform parameter (*m*) and phase shift of the channel (φ) on the axial velocity (*u*) are displayed in Figures 4 and 5. It is noted that the velocity profile *u* increases with a corresponding increase in *m* and opposite behavior observed for the phase shift φ.

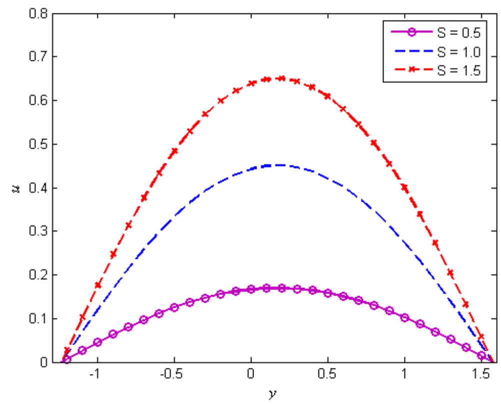

Figure 2. Variation of S on u for $a = 0.3$, $b = 0.5$, $\varphi = \pi/4$, $x = 0.5$, $m = 0.2$, $t = 0.2$.

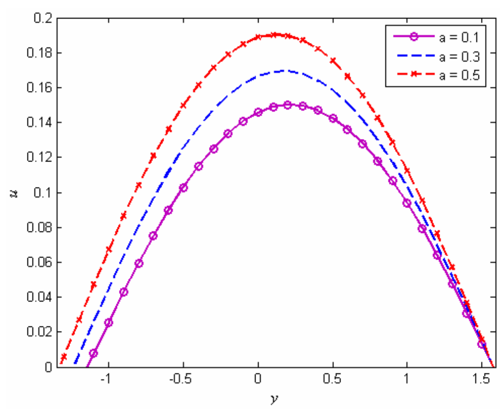

Figure 3. Variation of a on u for $b = 0.5$, $\varphi = \pi/4$, $x = 0.5$, $m = 0.2$, $t = 0.2$, $S = 0.5$.

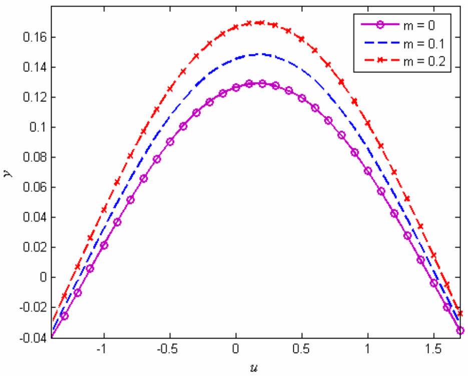

Figure 4. Variation of m on u for $a = 0.3$, $b = 0.5$, $\varphi = \pi/4$, $x = 0.5$, $t = 0.2$, $S = 0.5$.

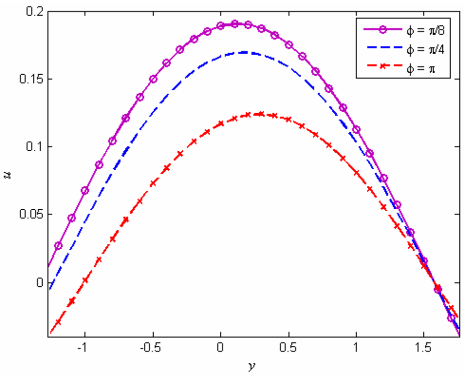

Figure 5. Variation of φ on u for $a = 0.3$, $b = 0.5$, $x = 0.5$, $m = 0.2$, $t = 0.2$, $S = 0.5$.

Heat transfer distributions

Figures 6-11 depict temperature profiles for several values of radiation parameter (R_n), Eckert number (E), Prandtl number (Pr), couple stress parameter (S), a non-uniform parameter (m) and amplitude of the lower wall (a). The influence of thermal radiation parameter (R_n) on temperature distribution θ is plotted in Figure 6. It is noted that the temperature distribution θ increases with decrease in R_n. The variation of Eckert number E on θ is shown in Figure 7. This figure shows that an increase in E results into an increase in θ. Figure 8 depicts the effect for various values of Prandtl number Pr.

From Figure 8, it is seen that the temperature θ increases as Prandtl number Pr increases. Figure 9 shows that the temperature profile θ increases with increase of couple stress parameter *S*. Figure 10 shows that the fluid temperature increases with an increase in non-uniform parameter (*m*). Figure 11 represents the temperature profile θ for various values of amplitude of lower wall *a*. It is clearly noticed that increasing *a* leads to increase in the fluid temperature θ.

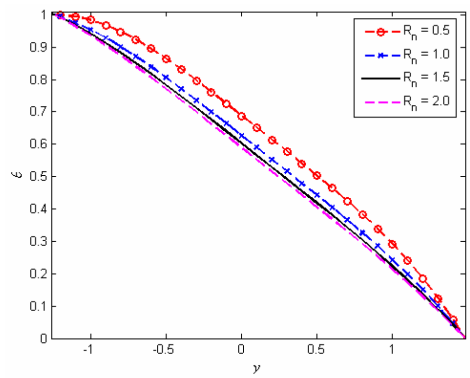

Figure 6. Variation of R_n on θ for $a = 0.3$, $b = 0.4$, $\varphi = \pi$, $x = 0.5$, $m = 0.2$, $t = 0.2$, $\Pr = 6.2$, $E = 0.75$, $S = 1.5$.

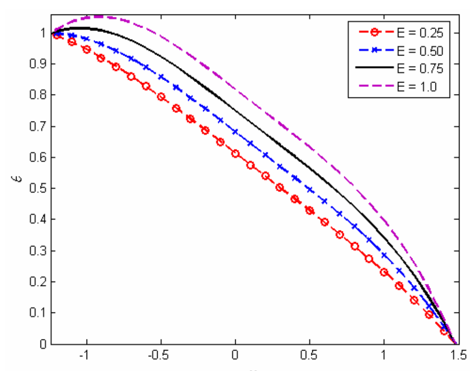

Figure 7. Variation of E on θ for $a = 0.3$, $b = 0.4$, $\varphi = \pi$, $x = 0.5$, $m = 0.2$, $t = 0.2$, $R_n = 0.3$, $\Pr = 6.2$, $S = 1.5$.

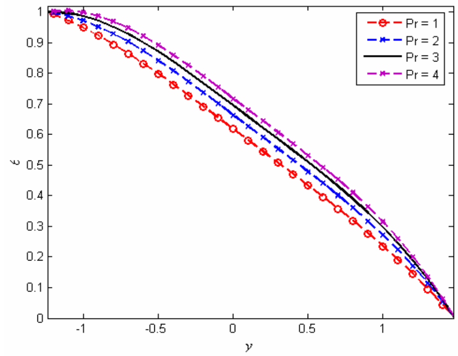

Figure 8. Variation of Pr on θ for $a = 0.3$, $b = 0.4$, $\varphi = \pi$, $x = 0.5$, $m = 0.2$, $t = 0.2$, $R_n = 0.3$, $E = 0.75$, $S = 1.5$.

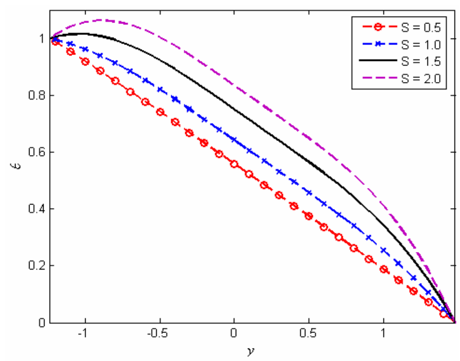

Figure 9. Variation of S on θ for $a = 0.3$, $b = 0.4$, $\varphi = \pi$, $x = 0.5$, $m = 0.2$, $t = 0.2$, $R_n = 0.3$, Pr = 6.2, $E = 0.75$.

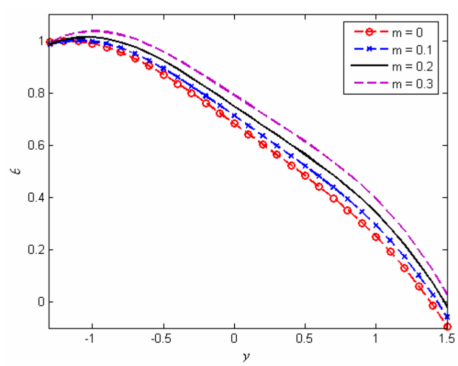

Figure 10. Variation of m on θ for $a = 0.3$, $b = 0.4$, $\varphi = \pi$, $x = 0.5$, $t = 0.2$, $R_n = 0.3$, Pr = 6.2, $E = 0.75$, $S = 1.5$.

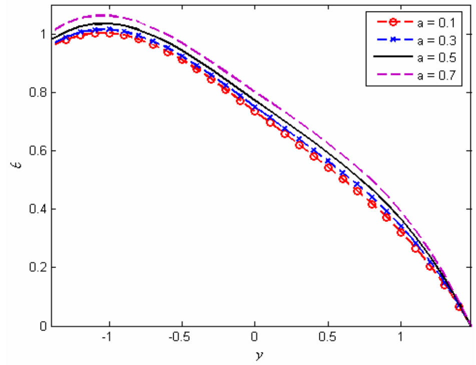

Figure 11. Variation of a on θ for $b = 0.4$, $\varphi = \pi$, $x = 0.5$, $m = 0.2$, $t = 0.2$, $R_n = 0.3$, $\Pr = 6.2$, $E = 0.75$, $S = 1.5$.

Conclusion

The present paper discussed the radiation effects on peristaltic transport of a couple stress fluid in a flexible tapered channel. Under the assumptions of large wavelength and low Reynolds number, analytic solutions have been derived for the amplitude of velocity and temperature. Effects of a variety of parameters with peristaltic transfer are also discussed. The main findings are summarized as follows:

1. The velocity profile increases with an increase in couple stress parameter, non-uniform parameter and amplitude of the lower wall.

2. The velocity of the fluid decreases with an increase in phase shift φ.

3. The temperature profile increases with an increase in Prandtl number Pr, Eckert number, couple stress parameter and non-uniform parameter m.

4. The temperature distribution decreases with increase in R_n.

References

[1] T. W. Latham, Fluid Motion in a Peristaltic Pump, MIT, Cambridge, 1966.

[2] A. H. Shapiro, M. Y. Jaffrin and S. L. Weinberg, Peristaltic pumping with long wave lengths at low Reynolds number, J. Fluid Mech. 37 (1969), 799-825.

[3] J. C. Burns and T. Parkes, Peristaltic motion, J. Fluid Mech. 29 (1967), 731-743.

[4] M. Kothandapani, J. Prakash and V. Pushparaj, Effects of heat transfer, magnetic field and space porosity on peristaltic flow of a Newtonian fluid in a tapered channel, Appl. Mech. Mater. 814 (2015), 679-684.

[5] J. G. Brasseur and S. Corrsin, The influence of a peripheral layer of different viscosity on peristaltic pumping with Newtonian fluids, J. Fluid Mech. 174 (1987), 495-519.

[6] D. J. Griffiths, Dynamics of the upper urinary tract: I. Peristaltic flow through a distensible tube of limited length, Physical Medical Biology 32 (1987), 813-822.

[7] T. Hayat, N. Alvi and N. Ali, Peristaltic mechanism of a Maxwell fluid in an asymmetric channel, Nonlinear Anal. Real World Appl. 9 (2008), 1474-1490.

[8] K. Vajravelu, G. Radhakrishnamacharya and V. R. Murty, Peristaltic flow and heat transfer in a vertical porous annulus with long wavelength approximation, Int. J. Nonlinear Mech. 42 (2007), 754-759.

[9] S. Nadeem, T. Hayat, N. S. Akbar and M. Y. Malik, On the influence of heat transfer in peristalsis with variable viscosity, Int. J. Heat Mass Trans. 52 (2009), 4722-4730.

[10] T. Hayat, M. U. Qureshi and Q. Hussain, Effect of heat transfer on the peristaltic flow of an electrically conducting fluid in a porous space, Appl. Math. Model. 33 (2009), 1862-1873.

[11] K. S. Mekheimer, S. Z. A. Husseny and Y. A. Elmaboud, Effects of heat transfer and space porosity on peristaltic flow in a vertical asymmetric channel, Numer. Methods Partial Diff. Eqs. 26 (2010), 747-770.

[12] S. Nadeem and N. S. Akbar, Effects of heat transfer on the peristaltic transport of MHD Newtonian fluid with variable viscosity: application of Adomian decomposition method, Commun. Nonlinear Sci. Numer. Simul. 14 (2009), 3844-3855.

[13] T. Hayat and S. Hina, The influence of wall properties on the MHD peristaltic flow of a Maxwell fluid with heat and mass transfer, Nonlinear Anal. Real World Appl. 11 (2010), 3155-3169.

[14] A. Ogulu, Effect of heat generation on low Reynolds number fluid and mass transport in a single lymphatic blood vessel with uniform magnetic field, Int. Commun. Heat Mass Trans. 33 (2006), 790-799.

[15] N. T. M. Eldabe, M. F. El-Sayed, A. Y. Ghaly and H. M. Sayed, Mixed convective heat and mass transfer in a non-Newtonian fluid at a peristaltic surface with temperature-dependent viscosity, Arch. Appl. Mech. 78 (2007), 599-624.

[16] S. Srinivas and M. Kothandapani, The influence of heat and mass transfer on MHD peristaltic flow through a porous space with compliant walls, Appl. Math. Comput. 213 (2009), 197-208.

[17] V. K. Stokes, Couple stresses in fluids, Phys. Fluids 9 (1966), 1709-1715.

[18] Kh. S. Mekheimer, Peristaltic transport of a couple stress fluid in a uniform and non-uniform channels, Biorheology 39(6) (2002), 755-765.

[19] S. Nadeem and S. Akram, Peristaltic flow of a couple-stress fluid under the effect of induced magnetic field in an asymmetric channel, Arch. Appl. Mech. 81 (2011), 97-109.

[20] Kh. S. Mekheimer, Effect of the induced magnetic field on peristaltic flow of a couple stress fluid, Physics Letters A 372 (2008), 4271-4278.

[21] O. Eytan, A. J. Jaffa and D. Elad, Peristaltic flow in a tapered channel: application to embryo transport within the uterine cavity, Medical Engineering & Physics 23 (2001), 473-482.

[22] M. Kothandapani, V. Pushparaj and J. Prakash, Effect of magnetic field on peristaltic flow of a fourth grade fluid in a tapered asymmetric channel, J. King Saud University - Engineering Sciences. Available online 5 January 2016. https://doi.org/10.1016/j.jksues.2015.12.009.

[23] M. Kothandapani, J. Prakash and V. Pushparaj, Analysis of heat and mass transfer on MHD peristaltic flow through a tapered asymmetric channel, J. Fluids 2015 (2015), Article ID 561263, 9 pp. http://dx.doi.org/10.1155/2015/561263.

[24] M. Kothandapani, V. Pushparaj and J. Prakash, Effects of slip and heat transfer on the magnetohydrodynamics peristaltic flow of a Jeffery fluid through a vertical tapered asymmetric channel, Global J. Pure Appl. Math. 12 (2016), 205-212.

[25] E. P. Siva and A. Govindarajan, Thermal radiation and Soret effect on MHD peristaltic transport through a tapered asymmetric channel with convective boundary conditions, Global J. Pure Appl. Math. 12 (2016), 213-221.